ORIGINAL PAPER

A Fractional Nonlinear Creep Damage Model for Transversely Isotropic Rock

Hao Kou[1] · Chuan He[1] · Wenbo Yang[1] · Fangyin Wu[1] · Zihan Zhou[1] · Jianfeng Fu[2] · Longge Xiao[3]

Abstract

Transversely isotropic layered rock is widely distributed in nature. To better describe the time-dependent entire creep characteristics for transversely isotropic rock, a simple nonlinear damage creep model is derived based on fractional order theory, which consists of a Hooke elastomer, a fractional Abel dashpot, a fractional nonlinear damage dashpot, and can effectively describe the characteristics of primary creep, steady-state creep and accelerating damage creep. Assuming that Poisson's ratio is constant, the creep equation of isotropic rock is extended to transversely isotropic rock, and the nonlinear damage creep model for transversely isotropic rock is established. Step-wise loading triaxial creep tests of phyllite specimens with three kinds of bedding angles (0°, 45° and 90°) are carried out, and it is found that there are significant differences in creep deformation and failure characteristics under different bedding angles. The parameters of the creep model at each bedding angle are identified using the Universal Global Optimization method. By comparing the Nishihara model, the modified Nishihara model and experimental data, it shows that the creep model in this paper are highly consistent with the experimental data under different bedding angles, load levels and creep stages, and the accuracy and rationality of the model are verified.

Highlights

- A simple nonlinear damage creep model is derived based on fractional order theory.
- By assuming that Poisson's ratio is constant, the creep equation of isotropic rock is extended to transversely isotropic rock, and the nonlinear damage creep model for transversely isotropic rock is established.

- There are significant differences in creep deformation and failure characteristics of phyllite specimens with different bedding angles.
- Parameters of the proposed creep model at each bedding angle are identified by using the Universal Global Optimization, and the accuracy and rationality of the model are verified.

✉ Wenbo Yang
yangwenbo1179@hotmail.com

1 Key Laboratory of Transportation Tunnel Engineering, Ministry of Education, Southwest Jiaotong University, Chengdu 610031, Si Chuan, China

2 Sichuan Mianjiu Expressway Co., Ltd., Chengdu 610041, Sichuan, China

3 China State Construction Engineering Corporation Co., Ltd., Beijing 100037, China

List of symbols

D	Damage variable
E	Elastic modulus parallel to foliation plane
E'	Elastic modulus perpendicular to foliation plane
G'	Shear modulus perpendicular to foliation plane
μ	Poisson's ratio parallel to foliation plane
μ'	Poisson's ratio perpendicular to foliation plane
m	Smallest integer greater than β
n	Ratio of E' to E
t	Creep time

t_a	Accelerating creep time
θ	Angle between loading direction and normal direction of bedding plane
β	Derivative order of visco-elastic body
γ	Derivative order of visco-plastic body
η	Viscosity coefficient
η_1	Viscosity coefficient of visco-elastic body
η_2	Viscosity coefficient of visco-plastic body
η_3	Viscosity coefficient of the nonlinear viscous body
λ	Damage parameter
σ	Axial stress
σ_s	Yield stress
ε	Axial strain
ε_e	Elastic strain
ε_{ve}	Visco-elastic strain
ε_{vp}	Visco-plastic strain
ε_a	Triggered strain of the accelerating creep stage
$\sigma_x, \sigma_y, \sigma_z$	Axial stresses in global coordinate system
$\tau_{yz}, \tau_{zx}, \tau_{xy}$	Tangential stresses in global coordinate system
$\varepsilon_x, \varepsilon_y, \varepsilon_z$	Axial strains in global coordinate system
$\gamma_{yz}, \gamma_{zx}, \gamma_{xy}$	Tangential strains in global coordinate system
$E_{\omega,\xi}(x)$	Mittag–Leffler function
$J(t)$	Creep compliance
$\Gamma(\beta)$	Gamma function
$[A]$	Poisson's ratio matrix for isotropic rock
$[U]$	Poisson's ratio matrix for transversely isotropic rock
$[S]$	Flexibility matrix of global coordinate system
$[S']$	Flexibility matrix of local coordinate system
$[\varepsilon]$	Strain tensor of global coordinate system
$[\varepsilon']$	Strain tensor of local coordinate system
$[\sigma]$	Stress tensor of global coordinate system
$[\sigma']$	Stress tensor of local coordinate system
s_{ij}	Components of matrix $[S]$
u_{ij}	Components of matrix $[U]$

1 Introduction

Layered rock masses are widely distributed in southwest China, such as phyllite, slate, shale, etc., which are obviously transversely isotropic (Aliabadian et al. 2019; Chen et al. 2017; Li et al. 2021a; Shen et al. 2021). With the rapid development of traffic construction in western China, more and more traffic tunnels need to cross the geological environment, especially in strata with extremely developed structural planes and bedding planes. Because of the low strength and strong rheological property of the surrounding rock, tunnels tend to suffer from asymmetric squeezing and large deformation (Chen et al. 2019; Liu et al. 2021b;

Sun et al. 2021; Xu et al. 2020). Therefore, it is of practical significance to investigate the creep behavior for layered rock masses.

Due to the existence of weak bedding planes, layered rocks often show obvious anisotropy characteristic, specifically transverse isotropic characteristic. Many scholars have studied the anisotropic/transversely isotropic characteristic and constitutive equation for layered rocks by theoretical or experimental method. Pouragha et al. (2020) regarded sandstone and slate as aggregates of cohesive particles, and described the strength anisotropy for layered rocks by combining local strength criterion and micromechanical equation of contact deformation. Saroglou and Tsiambaos (2008) and Shi et al. (2016) adopted the anisotropy exponents k_β and α_β respectively, and modified the Hoek–Brown criterion to describe the anisotropy of the triaxial strength for the layered rock. Wang et al. (2018b) established an elastic–plastic constitutive model for transversely isotropic rocks based on the Drucker–Prager criterion. Gholami and Rasouli (2014) used uniaxial, triaxial and Brazilian splitting tests to evaluate the mechanical parameters and strength properties of slates with different bedding directions, which have obvious U shaped distribution characteristics. However, the investigation for layered rocks mostly focuses on mechanical properties, strength characteristics, failure modes, etc., while there are few reports on its creep characteristics and creep constitutive model.

The research on rock creep constitutive model is still a hot spot in the field of rock mechanics at present. There are many kinds of creep constitutive models, which can be divided into three types: empirical models, component models and other nonlinear damage models based on fracture mechanics or damage mechanics. The classical component combination models are simple in form and clear in physical meaning, such as Burgers model, Nishihara model, which are widely used (Behbahani et al. 2016; Feng et al. 2021; Nomikos et al. 2011).
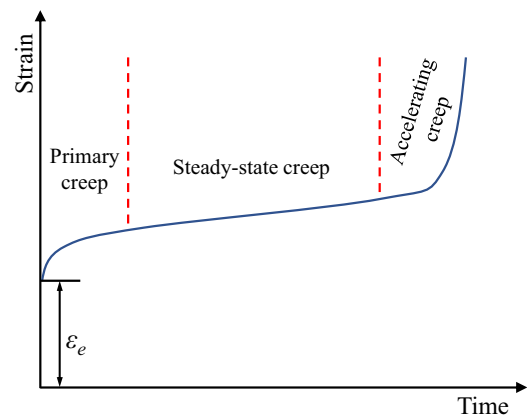

Fig. 1 Three stages of typical creep curve

However, the nonlinear accelerating creep stage of rock cannot be accurately described because the damage factor of the specimens is not considered (Fig. 1). To reflect the coupling phenomenon of rock damage and creep, many scholars modified the classical component combination model, such as Lin et al. (2020) modified Burgers model by adopting Kachanov creep damage law; Cheng et al. (2021) regarded rock as the material with microdefects or micro-damage, and proposed a nonlinear creep model based on modified Nishihara considering damage evolution; Feng et al. (2020) considered the initial damage and damage evolution, and improved the components in Nishihara model; Hou et al. (2019) researched different initial damage states of rock, and established a nonlinear damage model of four components, which consists of a Hooke body, a Kelvin body, an improved viscous component and a nonlinear viscous plastic damage component; Cao et al. (2020) derived a creep model including creep strengthening and weakening behaviors by introducing time-hardening theory and damage theory. In view of the fact that the above models are all integer orders, and there are some deviations in describing the characteristics of unsteady creep. Zhou et al. (2011) and Yan et al. (2020) proposed a creep model based on fractional derivative, by replacing Newtonian dashpot in Nishihara model with the fractional derivative Abel dashpot, to reflect the accelerating creep behavior of rock. Wu et al. (2021) described the complete creep process of salt rock by replacing Newtonian dashpot in Maxwell model with variable-order fractional derivative component. Xue et al. (2021) introduced the plastic damage variable and established Burgers model with the fractional damage creep to study the creep behavior of combined stress and temperature damage. Fractional order theory can express a variety of cases by the function of different orders, and can describe the visco-elastic and visco-plastic deformation behaviors more accurately, so it has become an important tool to describe creep behavior in recent years.

In the above researches, the rock mass is regarded as isotropic material, but the rock mass often has the properties of bedding, joints and structural planes, showing multi-layer anisotropy(Chen et al. 2016; Pouragha et al. 2020; Shen et al. 2021). Therefore, some scholars have studied the creep characteristics of transversely isotropic rock. Li et al. (2020) carried out four kinds of shale creep tests with different bedding angles (0°, 45°, 75° and 90°), and found that anisotropy had significant influence on the creep deformation and creep rate, among which the rock with bedding plane of 45° had the largest creep deformation and creep rate. The axial creep rate of carbonaceous slate in vertical bedding plane was higher than that in horizontal bedding plane (Wang et al. 2018c). By replacing the Newtonian component of Burgers model with the fractional derivative Abel dashpot, and introducing Poisson's ratio matrix of transversely isotropic rock, Li et al. (2021b) derived a creep constitutive model, which could describe the

steady-state creep for transversely isotropic rock. However, the existing models cannot adequately characterize the creep properties for transversely isotropic rock, especially the accelerating creep process.

To describe the accelerating creep process for transversely isotropic rock more truly and accurately, based on the fractional calculus theory, the fractional nonlinear damage creep model for isotropic rock was first derived with a simple form by introducing a damage variable D. Assuming that Poisson's ratio was constant, the Poisson's ratio of transversely isotropic rock was used to replace the Poisson's ratio in the proposed creep model, so the fractional nonlinear damage creep model for transversely isotropic rock was established. Through the step-wise loading triaxial creep tests of phyllite specimens with three kinds of bedding angles (0°, 45° and 90°), the creep characteristics of phyllite with different bedding angles were analyzed, and the reliability and accuracy of the model were verified.

2 Fractional Nonlinear Damage Creep Model

2.1 Definition of Fractional Calculus

Fractional calculus is developed on the basis of integral calculus, and many definitions have evolved (Lakshmikantham and Vatsala 2008). Among them, Riemann–Liouville (R–L) defined the fractional integral of a function $f(t)$ with order β ($0 \le \beta \le 1$), which is the most widely used, and the definition is as follows (Zhou et al. 2011):

$$\frac{d^{-\beta}[f(t)]}{dt^{-\beta}} = \frac{1}{\Gamma(\beta)} \int_0^t (t - \zeta)^{\beta-1} f(\zeta) d\zeta \tag{1}$$

where $\Gamma(\beta)$ is the gamma function and is defined as $\Gamma(\beta) = \int_0^\infty t^{\beta-1} e^{-t} dt$; ζ is an integral variable of $[0, t]$.

The fractional derivative of R-L is the inverse operation of fractional integral, then the fractional derivative of order β function $f(t)$ can be given by

$$\frac{d^\beta[f(t)]}{dt^\beta} = \frac{d^m}{dt^m}\left[\frac{d^{-(m-\beta)}[f(t)]}{dt^{-(m-\beta)}}\right] = \frac{1}{\Gamma(n-\beta)} \frac{d^m}{dt^m}\left[\int_0^t \frac{f(\zeta)}{(t-\zeta)^{\beta-m+1}} d\zeta\right] \tag{2}$$

where m is the smallest integer greater than β.

2.2 Fractional Abel Dashpot

Abel dashpot is a viscous component between ideal Hooke elastomer and Newtonian dashpot, a typical application of fractional calculus, which can reflect the nonlinear creep phenomenon of rock materials. The constitutive equation of an Abel dashpot is defined as (Zhou et al. 2011)

$$\sigma(t) = \eta \frac{d^\beta \varepsilon(t)}{dt^\beta}(0 \le \beta \le 1) \tag{3}$$

where η is the viscosity coefficient; $\sigma(t)$ is the axial stress and $\varepsilon(t)$ is the axial strain.

When $\beta = 0$, $\eta = E$, $\sigma = E\varepsilon$, representing linear elastomer, namely Hooke elastomer; When $\beta = 1$, $\sigma = \eta d\varepsilon/dt$, corresponding to Newtonian dashpot and satisfying the ideal fluid. Therefore, by adjusting the fractional order β, a satisfactory time-dependent strain curve can be obtained in the steady-state creep stage.

If $\sigma(t)$ is a constant stress, the Eq. (3) is integrated with R-L fractional operator, and the creep equation of fractional Abel dashpot can be expressed as follows:

$$\varepsilon(t) = \frac{d^{-\beta}}{dt^{-\beta}}\frac{\sigma}{\eta} = \frac{1}{\Gamma(\beta)}\int_0^t \frac{\sigma}{\eta}(t - \zeta)^{\beta-1}d\zeta = \frac{\sigma t^\beta}{\eta\Gamma(\beta+1)} \tag{4}$$

2.3 Fractional Nonlinear Damage Dashpot

The conventional fractional Abel dashpot cannot reflect the accelerating creep stage, which often happens in rock under high stress. To describe the phenomenon of accelerating creep, Xue et al. (2021) proposed the accelerating creep constitutive model for salt rock, the formula is as follows:

$$\sigma(t) = \eta \frac{d^\gamma \varepsilon(t)}{dt^\gamma}(\gamma \ge 1) \tag{5}$$

Several basic mechanical components are shown in Fig. 2. Considering the damage of rock during long-term loading, we introduce the damage variable D to describe the damage process. It is assumed that the probability of rock damage obeys the exponential distribution with parameter λ. The damage variable D can be described as (Chen et al. 2021)

$$D = \int_0^t \lambda e^{-\lambda t}dt = 1 - e^{-\lambda t} \tag{6}$$

where λ is the parameter to characterize the evolution law of time-dependent damage.

$$\sigma(t) = \eta(1 - D)\frac{d^\gamma \varepsilon(t)}{dt^\gamma} = \eta e^{-\lambda t}\frac{d^\gamma \varepsilon(t)}{dt^\gamma} \tag{7}$$

Considering $\sigma(t) = \sigma$, let $f(t) = \frac{\sigma}{\eta}e^{\lambda t}$, and $e^{\lambda t}$ can be expressed in the form of series as follows:

$$e^{\lambda t} = \sum_{i=0}^\infty \frac{(\lambda t)^i}{i!} = \sum_{i=0}^\infty \frac{(\lambda t)^i}{\Gamma(i+1)} \tag{8}$$

From Eqs. (1), (4) and (8), the creep equation of fractional nonlinear damage dashpot can be deduced as

$$\varepsilon(t) = \frac{d^{-\gamma}}{dt^{-\gamma}}\left[\sum_{i=0}^\infty \frac{\sigma(\lambda t)^i}{\eta\Gamma(i+1)}\right] = \sum_{i=0}^\infty \frac{\sigma\lambda^i t^{i+\gamma}}{\eta\Gamma(i+1+\gamma)} = \frac{\sigma t^\gamma}{\eta}E_{1,1+\gamma}(\lambda t) \tag{9}$$

where $E_{1,1+\gamma}(\lambda t)$ is Mittag–Leffler function, which is defined as

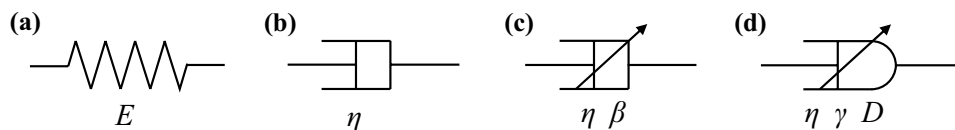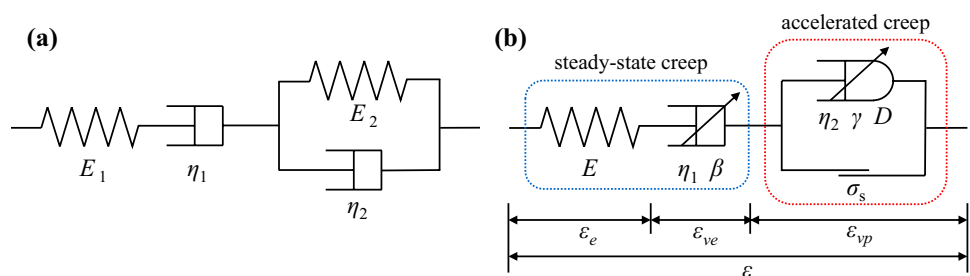$$E_{\omega,\xi}(x) = \sum_{i=0}^\infty \frac{x^i}{\Gamma(\omega i + \xi)} \tag{10}$$

Fig. 2 The basic mechanical components: a Hooke elastomer; b Newtonian dashpot; c fractional Abel dashpot; d fractional nonlinear damage dashpot

Fig. 3 Schematic view of creep constitutive model: a classical Burgers model; b fractional nonlinear damage creep Model

2.4 Establishment of the Fractional Nonlinear Damage Creep Model

The classical Burgers creep model consists of Hooke elastomer and Newtonian dashpot connected in series and in parallel (Fig. 3a), which can only reflect the creep characteristics of clay, asphalt and some rock, but cannot fully describe the creep process of rock, especially the accelerating creep stage (Behbahani et al. 2016; Lin et al. 2020). Therefore, we establish a fractional nonlinear damage creep model based on Burgers model, as shown in Fig. 3b. When the rock is in the steady-state creep stage without plastic yield, it can be described by the series connection of a Hooke elastomer and a fractional Abel dashpot, and the elastic deformation and visco-elastic deformation can be characterized, respectively. When the rock is in the accelerating creep stage with plastic flow, the fractional nonlinear damage dashpot is introduced to replace the Newtonian dashpot in Burgers model, and Hooke elastomer is substituted for a switch component. When $\sigma \geq \sigma_s$, the switch is active, and the nonlinear damage element starts to work to describe the visco-plastic deformation. This model can well describe the entire process of rock creep.

The above model is composed of a Hooke elastomer, a visco-elastic body and a visco-plastic body in series, and the corresponding strains are ε_e, ε_{ve} and ε_{vp} individually, so the total creep strain can be deduced as

$$\varepsilon = \varepsilon_e + \varepsilon_{ve} + \varepsilon_{vp} \tag{11}$$

Part 1. ε_e is the elastic strain, independent of time. It can be given as

$$\varepsilon_e = \frac{\sigma}{E} \tag{12}$$

Part 2. ε_{ve} is the visco-elastic strain, and the creep deformation derived from the fractional Abel dashpot Eq. (4) can be described as

$$\varepsilon_{ve} = \frac{\sigma t^\beta}{\eta_1 \Gamma(\beta + 1)} \tag{13}$$

where η_1 is the viscosity coefficient of visco-elastic body and β is the derivative order of visco-elastic body.

Part 3. ε_{vp} is the is visco-plastic strain, triggered by yield stress σ_s. The creep deformation obtained by the fractional nonlinear damage dashpot Eq. (9) can be expressed as

$$\varepsilon_{vp} = \begin{cases} 0, & \sigma < \sigma_s \\ \frac{\sigma t^\gamma}{\eta_2} E_{1,1+\gamma}(\lambda t), & \sigma \geq \sigma_s \end{cases} \tag{14}$$

where η_2 is the viscosity coefficient of visco-plastic body and γ is the derivative order of visco-plastic body.

By combine Eqs. (11)–(14), the fractional nonlinear damage creep model considering accelerating creep stage can be derived as

$$\varepsilon = \begin{cases} \frac{\sigma}{E} + \frac{\sigma t^\beta}{\eta_1 \Gamma(\beta+1)}, & \sigma < \sigma_s \\ \frac{\sigma}{E} + \frac{\sigma t^\beta}{\eta_1 \Gamma(\beta+1)} + \frac{\sigma t^\gamma}{\eta_2} E_{1,1+\gamma}(\lambda t), & \sigma \geq \sigma_s \end{cases} \tag{15}$$

Equation (15) gives the creep constitutive equations of steady-state creep and accelerating creep. When $\sigma < \sigma_s$, let $\sigma = 14$ MPa, $E = 11$ GPa, $\eta_1 = 20$ GPa·h$^\beta$, we draw a series of creep curves with different fractional orders β (Fig. 4a) and with different viscosity coefficients η_1 (Fig. 4b). It shows that the β is related to the creep rate and the η_1 is associated with the creep deformation. The larger β, the greater the creep rate, and the larger η_1, the smaller the creep deformation. When $\sigma \geq \sigma_s$, let $\sigma = 85$ MPa, $\eta_2 = 1$ GPa·h$^\gamma$, $\beta = 0.2$, $\lambda = 1$, we get a series of creep curves with different fractional orders γ (Fig. 4c) and with different viscosity coefficients η_2 (Fig. 4d). The γ represents the moment when the rock changes from the steady-state creep stage to the accelerating creep stage, and the larger γ, the later it will reach the accelerating creep failure state. The η_2 denotes the rate of accelerating creep, and the larger η_2, the steeper the curve. It shows that this model can well describe the characteristics of various creep stages of rock.

3 Fractional Nonlinear Damage Creep Model for Transversely Isotropic Rock

3.1 Fractional Nonlinear Damage Creep Model for Isotropic Rock

Let the creep compliance $J(t)$ in Eq. (15) is given as

$$J(t) = \begin{cases} \frac{1}{E} + \frac{t^\beta}{\eta_1 \Gamma(\beta+1)}, & \sigma < \sigma_s \\ \frac{1}{E} + \frac{t^\beta}{\eta_1 \Gamma(\beta+1)} + \frac{t^\gamma}{\eta_2} E_{1,1+\gamma}(\lambda t), & \sigma \geq \sigma_s \end{cases} \tag{16}$$

Then, Eq. (15) can be described as

$$\varepsilon = J(t)\sigma \tag{17}$$

Based on the creep constitutive equation established under one-dimensional condition, the equation can be extended from one-dimensional stress state to
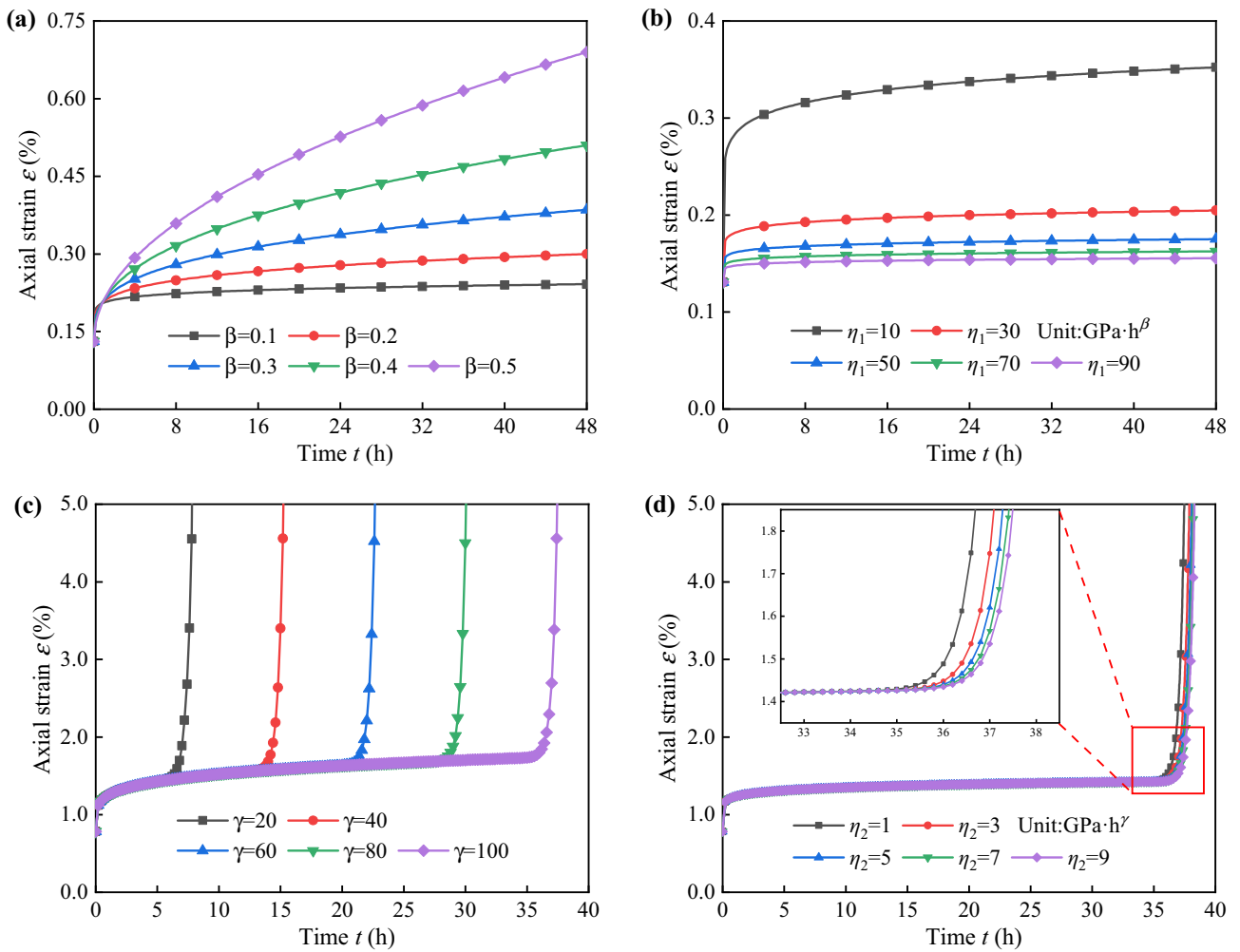
Fig. 4 Creep strain under different fractional orders: **a**, **b** steady-state creep stage ($\sigma < \sigma_s$); **c**, **d** accelerating creep stage ($\sigma \geq \sigma_s$)
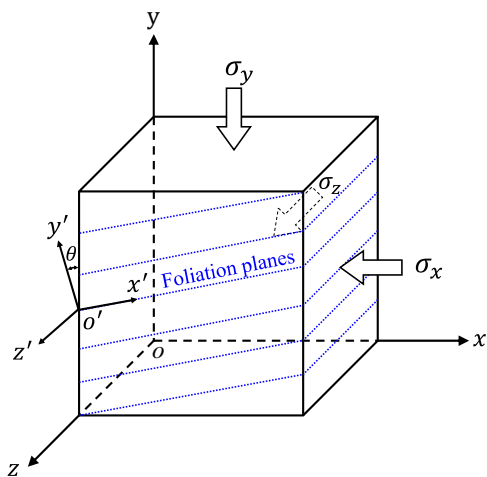

Fig. 5 Diagram of coordinate system for the transversely isotropic rock

three-dimensional. It is assumed that Poisson's ratio does not change with time and stress, and is equivalent to the value of elastic stage, $\mu(\sigma, t) = \mu$. For isotropic rock, the creep compliance substitution method can be used to obtain the basic form of the three-dimensional creep equation of rock as follows (Li et al. 2021b):

$$[\varepsilon] = J(t)[A][\sigma] \tag{18}$$

where $[A]$ is Poisson's ratio matrix for isotropic material; $[\varepsilon]$ and $[\sigma]$ are strain tensor and stress tensor, respectively.

3.2 Fractional Nonlinear Damage Creep Model for Transversely Isotropic Rock

For layered rock with transversely isotropic mechanical properties, as shown in Fig. 5, in the local coordinate

system $x'y'z'$, the stress–strain relationship for the transversely isotropic rock is as follows:

$$[\varepsilon'] = [S'][\sigma'] \tag{19}$$

Therein,

$$[S'] = \begin{bmatrix} \frac{1}{E} & -\frac{\mu'}{E'} & -\frac{\mu}{E} & 0 & 0 & 0 \\ -\frac{\mu'}{E'} & \frac{1}{E'} & -\frac{\mu'}{E'} & 0 & 0 & 0 \\ -\frac{\mu}{E} & -\frac{\mu'}{E'} & \frac{1}{E} & 0 & 0 & 0 \\ 0 & 0 & 0 & \frac{1}{G'} & 0 & 0 \\ 0 & 0 & 0 & 0 & \frac{2(1+\mu)}{E} & 0 \\ 0 & 0 & 0 & 0 & 0 & \frac{1}{G'} \end{bmatrix}$$

where $[\varepsilon']$, $[\sigma']$ and $[S']$ are strain tensor, stress tensor and flexibility matrix of local coordinate system, respectively; E and μ are elastic modulus and Poisson's ratio parallel to foliation plane, individually; E' and μ' and G' are elastic modulus, Poisson's ratio and shear modulus perpendicular to foliation plane, correspondingly.

According to the transformation relationship between local coordinates and global coordinates, Eq. (19) can be described as

$$[\varepsilon] = [Q][S'][Q]^{\mathrm{T}}[\sigma] \tag{20}$$

Therein,

$$[Q] = \begin{bmatrix} \cos^2\theta & \sin^2\theta & 0 & 0 & 0 & \frac{\sin 2\theta}{2} \\ \sin^2\theta & \cos^2\theta & 0 & 0 & 0 & -\frac{\sin 2\theta}{2} \\ 0 & 0 & 1 & 0 & 0 & 0 \\ 0 & 0 & 0 & \cos\theta & -\sin\theta & 0 \\ 0 & 0 & 0 & \sin\theta & \cos\theta & 0 \\ -\sin 2\theta & \sin 2\theta & 0 & 0 & 0 & \cos 2\theta \end{bmatrix}$$

The transversely isotropic rock has five independent elastic parameters. Gonzaga et al. (2008) reduced the independent elastic parameters to four, and put forward the approximate elastic parameters as follows:

$$\frac{1}{G'} = \frac{1}{E} + \frac{1}{E'} + \frac{2\mu'}{E'} \tag{21}$$

By matrix multiplication, Eq. (20) can be expressed as Eq. (22). Considering that the tangential stress is zero under conventional triaxial compression (Fig. 6), it can be further simplified as Eq. (23).
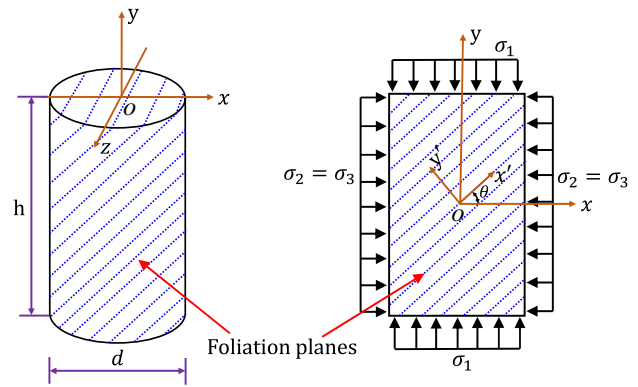

Fig. 6 Diagram of cylinder specimen for transversely anisotropic rock under confining pressure

$$\begin{Bmatrix} \varepsilon_x \\ \varepsilon_y \\ \varepsilon_z \\ \gamma_{yz} \\ \gamma_{zx} \\ \gamma_{xy} \end{Bmatrix} = \begin{bmatrix} s_{11} & s_{12} & s_{13} & s_{14} & s_{15} & s_{16} \\ s_{21} & s_{22} & s_{23} & s_{24} & s_{25} & s_{26} \\ s_{31} & s_{32} & s_{33} & s_{34} & s_{35} & s_{36} \\ s_{41} & s_{42} & s_{43} & s_{44} & s_{45} & s_{46} \\ s_{51} & s_{52} & s_{53} & s_{54} & s_{55} & s_{56} \\ s_{61} & s_{62} & s_{63} & s_{64} & s_{65} & s_{66} \end{bmatrix} \begin{Bmatrix} \sigma_x \\ \sigma_y \\ \sigma_z \\ \tau_{yz} \\ \tau_{zx} \\ \tau_{xy} \end{Bmatrix} \tag{22}$$

$$\begin{Bmatrix} \varepsilon_x \\ \varepsilon_y \\ \varepsilon_z \end{Bmatrix} = \begin{bmatrix} s_{11} & s_{12} & s_{13} \\ s_{21} & s_{22} & s_{23} \\ s_{31} & s_{32} & s_{33} \end{bmatrix} \begin{Bmatrix} \sigma_x \\ \sigma_y \\ \sigma_z \end{Bmatrix} \tag{23}$$

Assuming $E' = nE$ and combining Eq. (19), Eq. (20) and Eq. (21), s_{ij} can be expressed as

$$\begin{cases} s_{11} = \frac{1}{E}\left[\cos^4\theta + \sin^4\theta + \frac{\sin^2 2\theta}{4}\left(1 + \frac{1}{n}\right)\right] \\ s_{12} = s_{21} = -\frac{1}{E}\left(\frac{\mu'}{n}\sin^4\theta + \frac{\mu'}{n}\cos^4\theta + \frac{\mu'}{2n}\sin^2 2\theta\right) \\ s_{13} = s_{31} = -\frac{1}{E}\left(\mu\cos^2\theta + \frac{\mu'}{n}\sin^2\theta\right) \\ s_{22} = \frac{1}{E}\left[\sin^4\theta + \frac{\cos^4\theta}{n} + \frac{\sin^2 2\theta}{4}\left(1 + \frac{1}{n}\right)\right] \\ s_{23} = s_{32} = -\frac{1}{E}\left(\mu\sin^2\theta + \frac{\mu'}{n}\cos^2\theta\right) \\ s_{33} = \frac{1}{E} \end{cases}$$

The flexibility matrix can be written as

$$[S] = \frac{1}{E}[U] \tag{24}$$

$$[U] = \begin{bmatrix} u_{11} & u_{12} & u_{13} \\ u_{21} & u_{22} & u_{23} \\ u_{31} & u_{32} & u_{33} \end{bmatrix}$$

Fig. 7 Fractional components for transversely isotropic rock: **a** fractional Abel dashpot; **b** fractional nonlinear damage dashpot
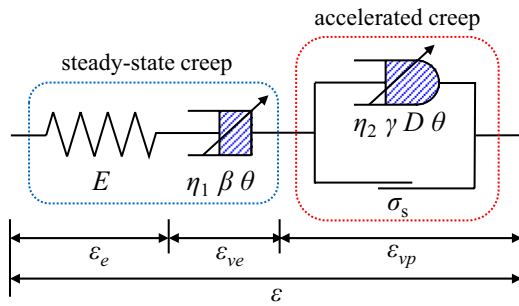

Fig. 8 Schematic view of fractional nonlinear damage creep model for transversely isotropic rock

$$\begin{cases} u_{11} = \cos^4\theta + \sin^4\theta + \frac{\sin^2 2\theta}{4}\left(1 + \frac{1}{n}\right) \\ u_{12} = u_{21} = -\frac{\mu'}{n}\left(\sin^4\theta + \cos^4\theta + \frac{\sin^2 2\theta}{2}\right) \\ u_{13} = u_{31} = -\left(\mu\cos^2\theta + \frac{\mu'}{n}\sin^2\theta\right) \\ u_{22} = \sin^4\theta + \frac{\cos^4\theta}{n} + \frac{\sin^2 2\theta}{4}\left(1 + \frac{1}{n}\right) \\ u_{23} = u_{32} = -\left(\mu\sin^2\theta + \frac{\mu'}{n}\cos^2\theta\right) \\ u_{33} = 1 \end{cases}$$

Using differential operator substitution method, keeping Poisson's ratio matrix unchanged, and replacing Poisson's ratio matrix $[A]$ of the isotropic rock in Eq. (18) with Poisson's ratio matrix $[U]$ of the transversely isotropic rock shown in Eq. (24), the three-dimensional creep constitutive equation for transversely anisotropic rock can be obtained as follows:

$$[\varepsilon] = J(t)[U][\sigma] \tag{25}$$

Therefore, the fractional Abel dashpot and fractional nonlinear damage dashpot considering bedding angle can be shown as Fig. 7. The fractional nonlinear damage creep model for transversely isotropic rock can be represented as Fig. 8. It can embody the instantaneous elastic, steady-state creep visco-elastic and accelerating creep visco-plastic deformation of rock with different bedding angles. The creep deformation can be obtained by expanding Eq. (25), and the axial creep equation is shown as follows:

If $\sigma < \sigma_s$, then:

$$\begin{aligned} \varepsilon_y = \left(\frac{1}{E} + \frac{t^\beta}{\eta_1 \Gamma(\beta+1)}\right) &\left\{ -\frac{\mu'}{n}\left(\sin^4\theta + \cos^4\theta + \frac{\sin^2 2\theta}{2}\right)\sigma_x \right. \\ &+ \left[\sin^4\theta + \frac{\cos^4\theta}{n} + \frac{\sin^2 2\theta}{4}\left(1 + \frac{1}{n}\right)\right]\sigma_y \\ &\left. - \left(\mu\sin^2\theta + \frac{\mu'}{n}\cos^2\theta\right)\sigma_z \right\} \end{aligned} \tag{26}$$

If $\sigma \geq \sigma_s$, then:

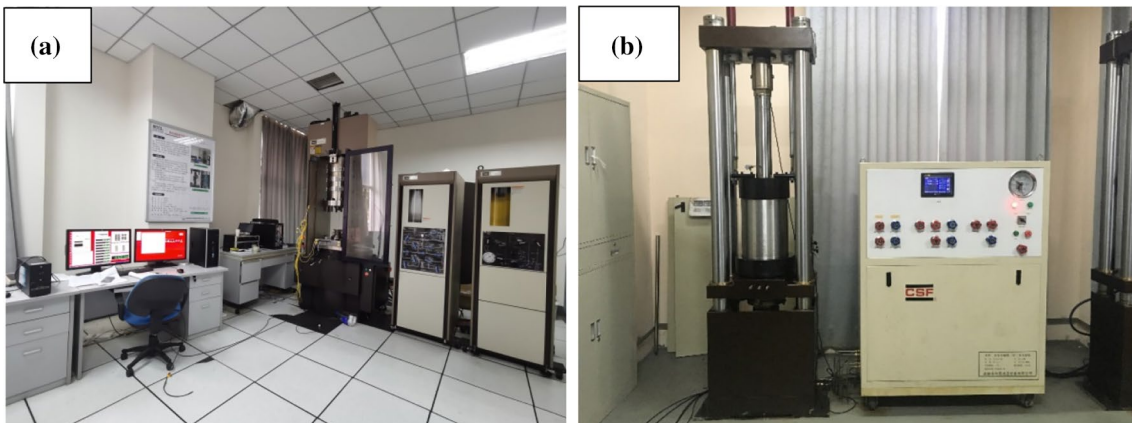Fig. 9 Experimental equipment: **a** MTS815 rock servo-controlled equipment; **b** Rock triaxial rheological equipment
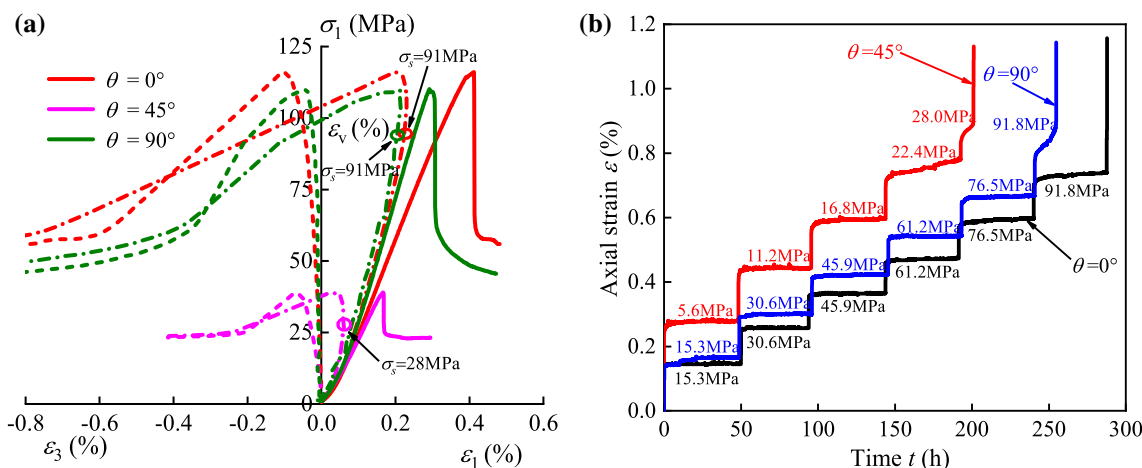
Fig. 10 Experimental data of phyllite with different bedding angles: **a** Triaxial compression test, $\sigma_3 = 10$ MPa; **b** Triaxial creep test, $\sigma_3 = 10$ MPa

$$\varepsilon_y = \left(\frac{1}{E} + \frac{t^\beta}{\eta_1 \Gamma(\beta+1)} + \frac{t^\gamma}{\eta_2} E_{1,1+\gamma}(\lambda t) \right) \left\{ -\frac{\mu'}{n}\left(\sin^4\theta + \cos^4\theta + \frac{\sin^2 2\theta}{2} \right)\sigma_x + \left[\sin^4\theta + \frac{\cos^4\theta}{n} + \frac{\sin^2 2\theta}{4}\left(1 + \frac{1}{n}\right) \right]\sigma_y - \left(\mu\sin^2\theta + \frac{\mu'}{n}\cos^2\theta \right)\sigma_z \right\}$$

(27)

4 Model Verification Based on Triaxial Creep Test for Layered Phyllite

4.1 Triaxial Creep Test for Layered Phyllite

We prepared phyllite rock specimens with a diameter of 50 mm, a height of 100 mm and bedding angles of 0°, 45° and 90° respectively. First, the triaxial compression test with the circumferential stress of 10 MPa was carried out on the phyllite specimens using MTS815 rock servo-controlled equipment (Fig. 9a). As shown in the stress–strain curve in Fig. 10a, the strength of $\theta = 0°$ and $\theta = 90°$ rock specimens were similar and higher, while that of $\theta = 45°$ rock specimen was lower, and the strength of phyllite showed obvious anisotropy. According to the method to determine the yield stress, we set the stress at the inflection point of the volume stress–strain curve as the yield stress (Liu et al. 2021a). The yield stress of $\theta = 0°$ and $\theta = 90°$ rock specimens was 91 MPa, and the yield stress of $\theta = 45°$ rock specimen was 28 MPa. Then, according to the obtained yield stress, the creep test of the same circumferential stress was carried out using the rock triaxial

rheological equipment (Fig. 9b). We adopted the method of multi-stage loading, each stage of loading lasted for 48 h, divided equally according to the yield stress, and the rock specimens are loaded step by step until they failed.

The creep curves of the phyllite specimens with three kinds of bedding angles are shown in Fig. 10b. There are obvious differences in creep characteristics of phyllite with
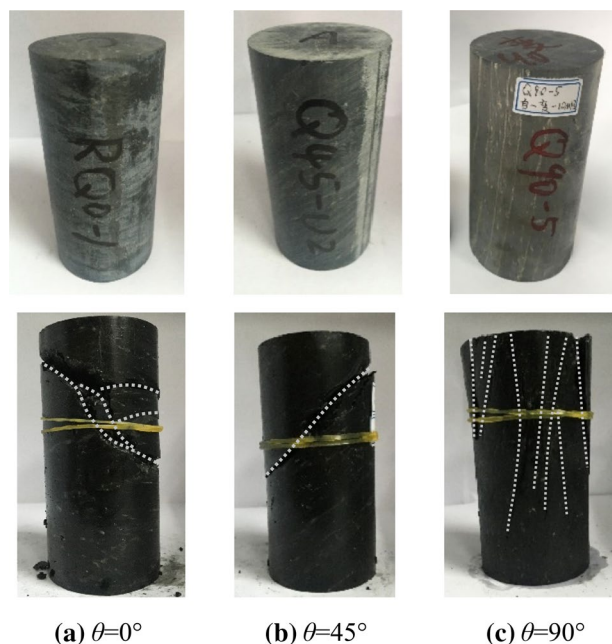
Table 1 Elastic parameters of phyllite

E (GPa)	E' (GPa)	G' (GPa)	μ	μ'
26.55	29.31	10.38	0.29	0.36

Fig. 11 Failure characteristics of phyllite: **a** $\theta = 0°$; **b** $\theta = 45°$; **c** $\theta = 90°$

Table 2 Fitted parameters of fractional nonlinear damage creep model for phyllite

Bedding angles	β	η_1 (GPa h$^\beta$)	γ	η_2 (GPa h$^\gamma$)	λ
$\theta = 0°$	0.023	23.56	137.94	1.67	3.78
$\theta = 45°$	0.024	3.98	23.97	4.26	1.08
$\theta = 90°$	0.036	22.81	45.75	1.04	4.44

different bedding angles. Overall, when $\theta = 45°$, the deformation is the largest, when $\theta = 0°$, the deformation is the smallest, and when $\theta = 90°$, the deformation is in between. In the first few stages of loading, the specimens were in the steady-state creep, which consists of transient and time-dependent deformation. In the last stage of loading, the specimens entered the state of nonlinear accelerating creep and failed. The accelerating creep process of phyllite with bedding angle of 45° and 90° is more obvious and the duration is shorter, while the accelerating creep curve with bedding angle of 0° is steeper and the duration is longer.

The failure characteristics of the phyllite specimens are quite different (Fig. 11). The time-dependent deformation process of phyllite is explained from the failure mechanism. When $\theta = 0°$, the rock is subjected to combined tensile–shear failure through bedding and parallel bedding planes, and the deformation is controlled by the weak plane of horizontal bedding, which is relatively large, and the accelerating creep occurs later. When $\theta = 90°$, the rock is subjected to splitting tension parallel to bedding planes, and the deformation is dominated by vertical matrix, which is relatively small, and the accelerating creep occurs earlier. When $\theta = 45°$, the rock shears and slips along the weak bedding plane, with the largest deformation and the earliest accelerating creep. There are significant differences in phyllite failure modes with different bedding angles.

4.2 Parameter Identification and Model Verification

The elastic parameters of phyllite obtained from rock mechanics experiments are shown in Table 1. According to the triaxial creep data of layered phyllite, the parameters of the fractional nonlinear damage creep model with each bedding angle are identified by Universal Global Optimization (Table 2). To show the influence of bedding direction on model parameters more clearly, we get the approximate relationship between the model parameters and bedding angles by polynomial fitting for better practical application (Fig. 11). With the increase of bedding angle, the fractional order β becomes larger, and the viscous parameter η_1, the fractional order γ, the parameter λ first decrease and then increase, and the viscous parameter η_2 first increase and then

decrease. According to the fitted curve relationship, we can roughly get the model parameters β, η_1, γ, η_2 and λ, corresponding to other bedding angles (Fig. 12).

By bringing the above identified parameters into Eqs. (26) and (27), the calculation curves of time-dependent creep deformation for three kinds of bedding angles under different load levels can be obtained. The comparisons between experimental data and calculation curves are shown in Fig. 13. The fractional nonlinear damage creep model for transversely isotropic rock can not only reflect the deformation law of layered rock in the steady-state creep, but also describe the nonlinear accelerating deformation characteristics in the accelerating creep stage. The calculated curves are highly consistent with the experimental data under different bedding angles, load levels and creep stages, which shows that the model is accurate and reasonable.

To better verify this model, it is compared with the classical Nishihara model and the modified Nishihara model with damage which can describe the accelerating creep (Wang et al. 2018a, 2021) (Fig. 14). Equation (28) is the creep equation of Nishihara model, and Eq. (29) is the creep equation of Nishihara model modified by Wang et al. (2018a), as follows:

$$\begin{cases} \varepsilon(t) = \frac{\sigma}{E_1} + \frac{\sigma}{E_2}\left(1 - e^{-(E_2/\eta_1)t}\right), & \sigma < \sigma_s \\ \varepsilon(t) = \frac{\sigma}{E_1} + \frac{\sigma}{E_2}\left(1 - e^{-(E_2/\eta_1)t}\right) + \frac{\sigma - \sigma_s}{\eta_2}, & \sigma \geq \sigma_s \end{cases} \quad (28)$$

where E_1 is the instantaneous elastic modulus, E_2 is the visco-elastic modulus, η_1 and η_2 are the viscosity coefficients.

$$\begin{cases} \varepsilon(t) = \frac{\sigma}{E_1} + \frac{\sigma}{E_2}\left(1 - e^{-(E_2/\eta_1)t}\right), & \sigma < \sigma_s \\ \varepsilon(t) = \frac{\sigma}{E_1} + \frac{\sigma}{E_2}\left(1 - e^{-(E_2/\eta_1)t}\right) + \frac{\sigma - \sigma_s}{\eta_2}, & \sigma \geq \sigma_s, \varepsilon < \varepsilon_a \\ \varepsilon(t) = \frac{\sigma}{E_1} + \frac{\sigma}{E_2}\left(1 - e^{-(E_2/\eta_1)t}\right) + \frac{(\sigma - \sigma_s)(1 - D)}{\eta_2}t + \frac{\sigma}{\eta_3}(t - t_a), & \sigma \geq \sigma_s, \varepsilon \geq \varepsilon_a \end{cases}$$
$$(29)$$

where η_3 is the viscosity coefficient of the nonlinear viscous dashpot, ε_a is the triggered strain of accelerating creep stage, t_a is the time corresponding to the strain ε_a, D is the damage variable, the same as Eq. (6), $D = 1 - e^{-\lambda t}$.

The parameters of the modified Nishihara model were obtained by fitting the phyllite creep experimental data, as shown in Table 3. By substituting the parameters into Eq. (28), the calculation curves for the primary creep and steady-state creep stages can be drawn (Fig. 15). Comparing the fractional nonlinear damage creep model in this paper, it is found that the both describe the creep process well under low stress conditions. However, as the stress increases, the
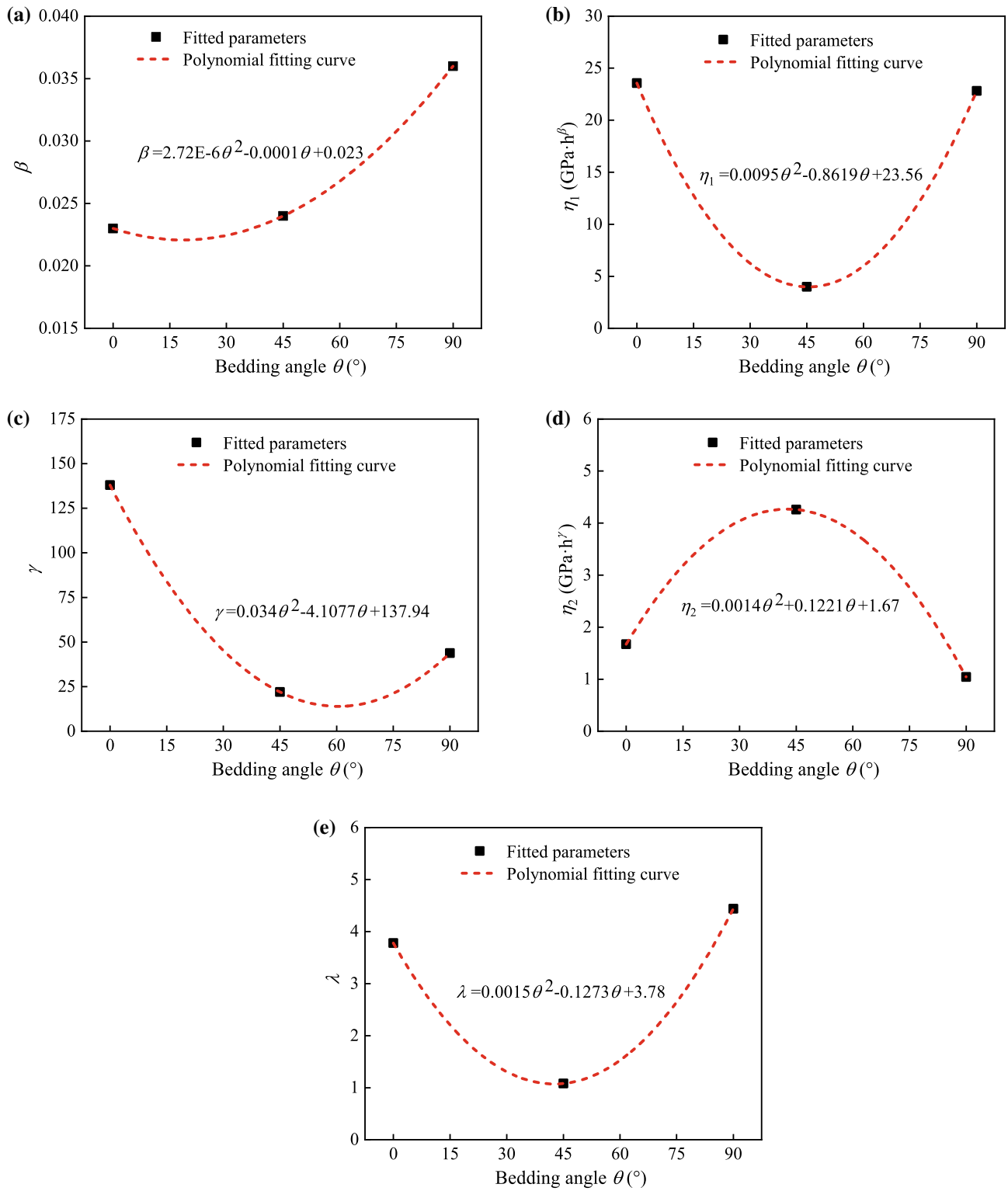
Fig. 12 Fitted parameters and polynomial fitting curve: **a** β; **b** η_1; **c** γ; **d** η_2; **e** λ

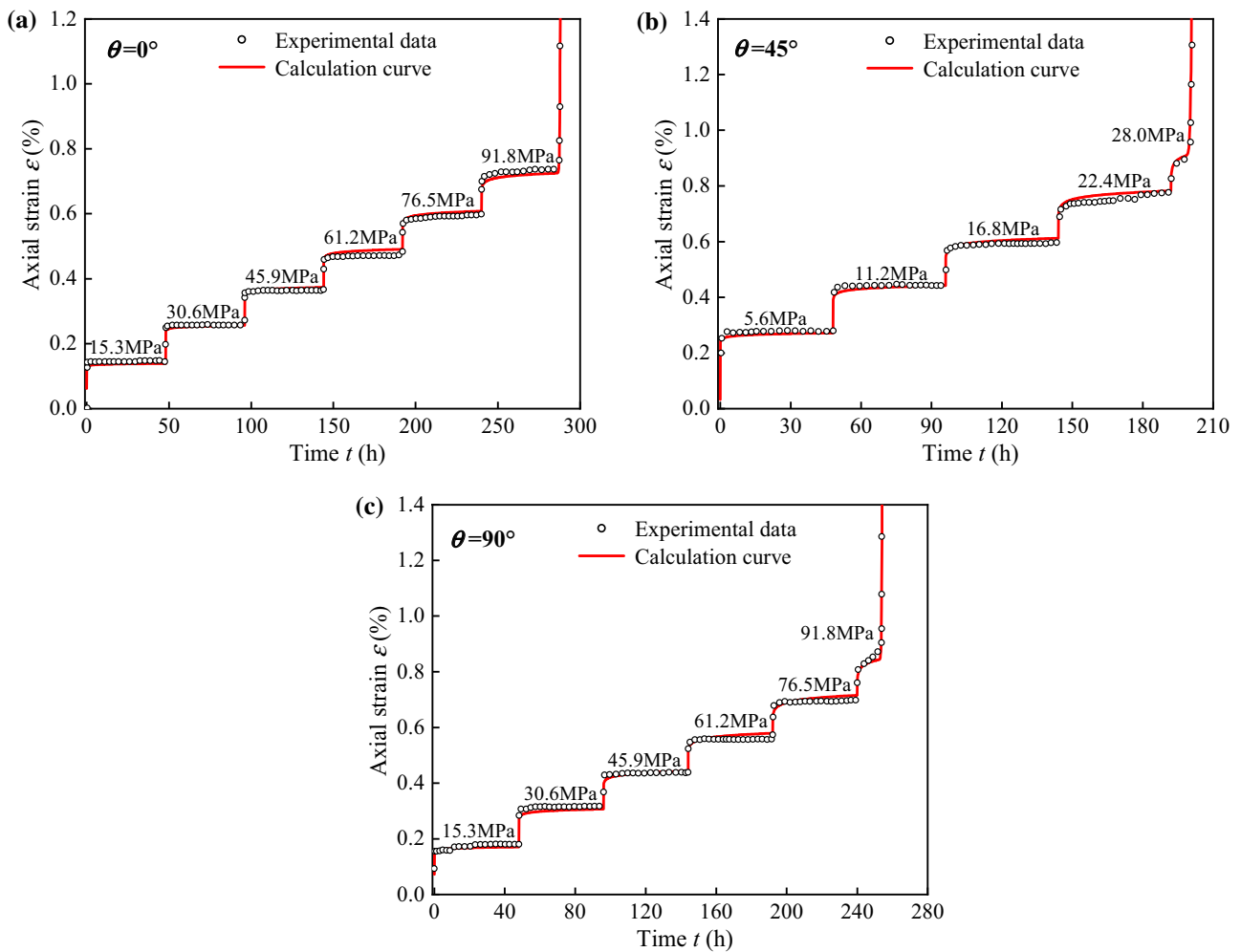**Fig. 13** Comparison between experimental data and calculation curve: **a** $\theta=0°$; **b** $\theta=45°$; **c** $\theta=90°$

difference between the calculated results of the Nishihara model and the experimental data becomes larger and larger, which is mainly reflected in the primary creep stage. The fractional nonlinear damage creep model in this paper also describes the creep process well under high stress conditions, and the fitting results are good.

Similarly, by substituting the parameters into Eq. (29), the calculation curves of the accelerating creep stage can be obtained (Fig. 16). We compare the calculation curves of the Nishihara model, the modified Nishihara model, and the fractional nonlinear damage model in this paper. It shows

that the classical Nishihara model cannot reflect the accelerating creep process. Although the modified Nishihara model could describe the accelerating creep process, it is relatively different from the experimental results, and the nonlinear deformation process is poorly described. Moreover, it is necessary to determine the time when accelerating creep occurs, which is not practical and has many parameters. The fractional nonlinear damage creep model in this paper is simple, and the entire nonlinear accelerating creep process can be described clearly with five simple parameters.

Table 3 Fitted parameters of the modified Nishihara model for phyllite

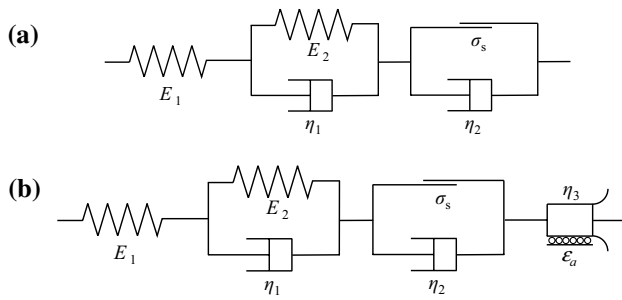| Bedding angles	E_1 (GPa)	E_2 (GPa)	η_1 (GPa h)	η_2 (GPa h)	η_3 (GPa h)	λ	t_a
$\theta=0°$	26.55	21.69	2.88	222	22.4	3.78	47.3
$\theta=45°$	27.86	3.62	0.47	220	9.3	1.08	7.9
$\theta=90°$	29.31	20.00	2.13	576	21.6	4.44	13.0

Fig. 14 Schematic view of Nishihara model: **a** classical Nishihara model; **b** modified Nishihara model
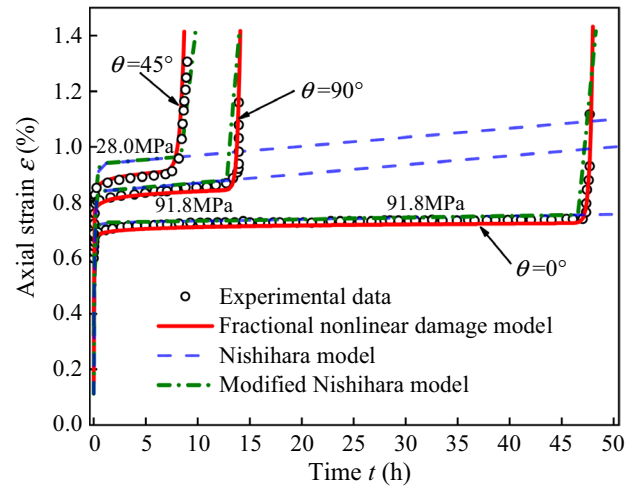

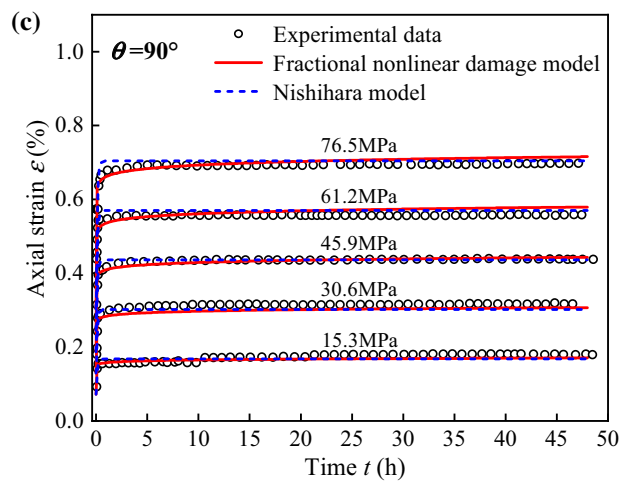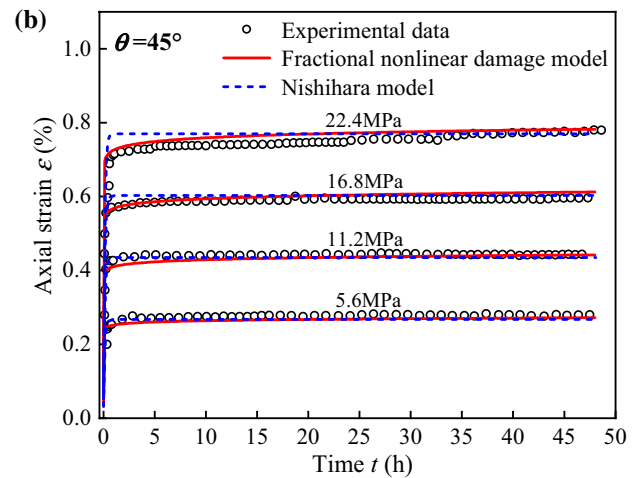Fig. 16 Comparison with the Nishihara model and the modified Nishihara model in the accelerating creep stage

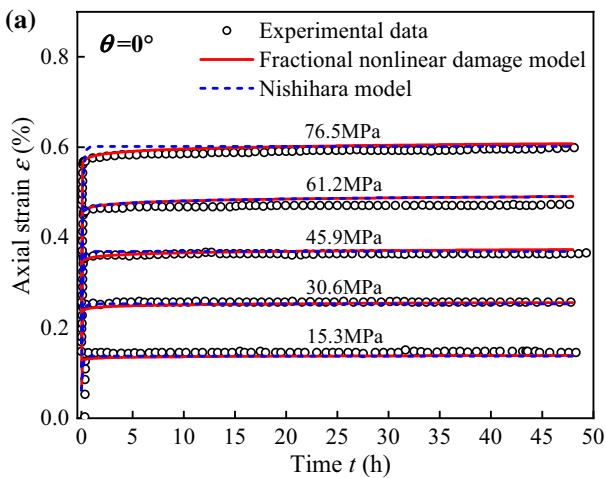Fig. 15 Comparison with the Nishihara model in the primary creep and steady-state creep stages: **a** $\theta = 0°$; **b** $\theta = 45°$; **c** $\theta = 90°$
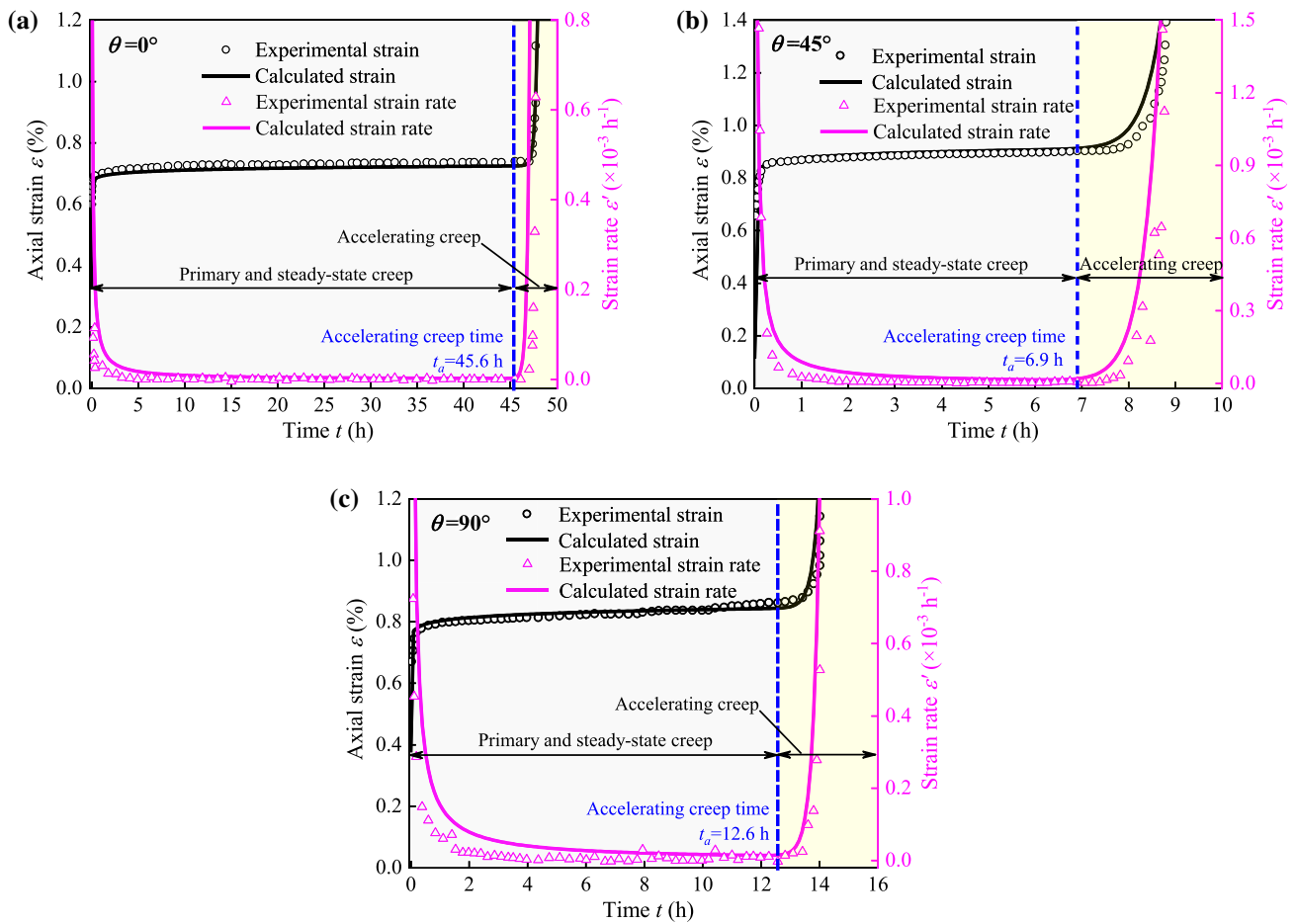
Fig. 17 The accelerating creep time: **a** $\theta = 0°$; **b** $\theta = 45°$; **c** $\theta = 90°$

5 Discussion

The creep model in this paper was verified and its parameters were identified, and it was also compared with the Nishihara model and the modified Nishihara model with damage. The modified Nishihara model could not describe the nonlinear process of accelerating creep well, and the accelerating creep time needed to be fitted. In this paper, the combination of fractional derivative, transversely isotropic constitutive model and damage variable could better describe the nonlinear accelerating creep process for layered rock, and the accelerating creep time could also be determined by taking the derivative of the creep equation as 0. The creep rate is calculated as follows:

$$\varepsilon'_y = \left(\frac{\beta t^{\beta-1}}{\eta_1 \Gamma(\beta+1)} + \frac{\gamma t^{\gamma-1}}{\eta_2} E_{1,1+\gamma}(\lambda t) + \frac{\lambda t^\gamma}{\eta_2} E_{1,1+\gamma}(\lambda t) \right)$$

$$\left\{ -\frac{\mu'}{n} \left(\sin^4 \theta + \cos^4 \theta + \frac{\sin^2 2\theta}{2} \right) \sigma_x \right.$$

$$\left. + \left[\sin^4 \theta + \frac{\cos^4 \theta}{n} + \frac{\sin^2 2\theta}{4} \left(1 + \frac{1}{n} \right) \right] \sigma_y - \left(\mu \sin^2 \theta + \frac{\mu'}{n} \cos^2 \theta \right) \sigma_z \right\}$$

$$\tag{30}$$

The above fitted creep parameters of phyllite rocks with different bedding angles are substituted into Eq. (30), and the relationship curves of strain rate with time are calculated respectively. As shown in Fig. 17, it clearly shows that the strain rate begins to increase rapidly after reaching the minimum value, which indicates that accelerating creep begins to occur. The time-dependent strain rate curve is basically consistent with the experimental strain rate, and the accelerating creep time for bedding angles of 0°, 45°, 90° are 45.6, 6.9, 12.6 h respectively, which indicates that this method can determine the accelerating creep time. Compared with the modified Nishihara model, the accelerating creep time by this method is earlier and the result is more accurate.

6 Conclusion

Based on fractional calculus, a nonlinear creep damage model for transversely isotropic rock is established and its analytical solution is given. Through step-wise loading triaxial creep tests on phyllite specimens with three kinds of

bedding angles of 0°, 45° and 90°, the parameters of the proposed creep model are identified and verified, and the creep deformation characteristics of rock with different bedding angles are analyzed. The major conclusions are as follows:

1. Based on fractional calculus and introducing the damage variable D, a fractional nonlinear creep damage model is established, which can describe the accelerating creep process of isotropic rock. Sensitivity analysis of the creep model parameters shows that the fractional order β is positively related to the creep rate, and the viscosity coefficient η_1 is negatively associated with the creep deformation; The fractional order γ represents the moment when the accelerating creep state occurs, and the larger it is, the later it will be; The viscosity coefficient η_2 is positively correlated with the speed of accelerating creep.

2. Assuming that Poisson's ratio is constant, the Poisson's ratio matrix of transversely isotropic rock is substituted for the Poisson's ratio matrix of the three-dimensional creep equation expressed by the nonlinear damage creep model, so as to establish the fractional nonlinear damage creep model for transversely isotropic rock. It can effectively describe the characteristics of primary creep, steady-state creep and accelerating creep of layered rock with different bedding angles.

3. Through the triaxial creep test for phyllite, it is found that the creep deformation and failure characteristics of rock with different bedding angles are significantly different. When $\theta = 0°$, the rock is subjected to combined tensile–shear failure through bedding and parallel bedding planes, with moderate deformation and the latest acceleration of creep. When $\theta = 45°$, the shear slip failure of the rock along the bedding plane leads to the largest deformation and the earliest accelerating creep. When $\theta = 90°$, the rock is subjected to splitting tensile failure parallel to bedding plane, with the smallest deformation and earlier accelerating creep time.

4. According to the experimental data, the parameters of the fractional nonlinear damage creep model are identified by Universal Global Optimization. By comparing the experimental data with the calculation curve, it is shown that the calculation curves are highly consistent with the experimental data under different bedding angles, load levels and creep stages. Compared with the Nishihara model and the modified Nishihara model, the fractional nonlinear damage creep model established in this paper can better describe the creep and nonlinear accelerating creep process under high stress conditions, and the fitting effect is good, which indicates that the model is accurate and reasonable. In addition, the creep model in this paper can also determine the time of accelerating creep.

Declarations

Conflict of interest The authors declare that we have no conflict of interest.

References

Aliabadian Z, Zhao GF, Russell AR (2019) Failure, crack initiation and the tensile strength of transversely isotropic rock using the brazilian test. Int J Rock Mech Min Sci. https://doi.org/10.1016/j.ijrmms.2019.104073

Behbahani H, Ziari H, Kamboozia N (2016) Evaluation of the visco-elasto-plastic behavior of glasphalt mixtures through generalized and classic burger's models modification. Constr and Build Mater 118:36–42. https://doi.org/10.1016/j.conbuildmat.2016.04.157

Cao WG, Chen K, Tan X et al (2020) A novel damage-based creep model considering the complete creep process and multiple stress levels. Comput and Geotech. https://doi.org/10.1016/j.compgeo.2020.103599

Chen YF, Wei K, Liu W et al (2016) Experimental characterization and micromechanical modelling of anisotropic slates. Rock Mech Rock Eng 49:3541–3557. https://doi.org/10.1007/s00603-016-1009-x

Chen ZQ, He C, Wu D et al (2017) Fracture evolution and energy mechanism of deep-buried carbonaceous slate. Acta Geotech 12:1243–1260. https://doi.org/10.1007/s11440-017-0606-5

Chen ZQ, He C, Xu GW et al (2019) A case study on the asymmetric deformation characteristics and mechanical behavior of deep-buried tunnel in phyllite. Rock Mech Rock Eng 52:4527–4545. https://doi.org/10.1007/s00603-019-01836-2

Chen G, Wan Y, Sun X et al (2021) Research on creep behaviors and fractional order damage model of sandstone subjected to freeze-thaw cycles in different temperature ranges. Chin J Rock Mech Eng 40:1962–1975

Cheng H, Zhang YC, Zhou XP (2021) Nonlinear creep model for rocks considering damage evolution based on the modified nishihara model. Int J Geomech. https://doi.org/10.1061/(asce)gm.1943-5622.0002071

Feng WL, Qiao CS, Niu SJ et al (2020) An improved nonlinear damage model of rocks considering initial damage and damage evolution. Int J Damage Mec 29:1117–1137. https://doi.org/10.1177/1056789520909531

Feng YY, Yang XJ, Liu JG et al (2021) A new fractional nishihara-type model with creep damage considering thermal effect. Eng Fract Mech. https://doi.org/10.1016/j.engfracmech.2020.107451

Gholami R, Rasouli V (2014) Mechanical and elastic properties of transversely isotropic slate. Rock Mech Rock Eng 47:1763–1773. https://doi.org/10.1007/s00603-013-0488-2

Gonzaga GG, Leite MH, Corthesy R (2008) Determination of anisotropic deformability parameters from a single standard rock

specimen. Int J Rock Mech Min Sci 45:1420–1438. https://doi.org/10.1016/j.ijrmms.2008.01.014

Hou RB, Zhang K, Tao J et al (2019) A nonlinear creep damage coupled model for rock considering the effect of initial damage. Rock Mech Rock Eng 52:1275–1285. https://doi.org/10.1007/s00603-018-1626-7

Lakshmikantham V, Vatsala AS (2008) Basic theory of fractional differential equations. Nonlinear Anal-Theor 69:2677–2682. https://doi.org/10.1016/j.na.2007.08.042

Li CB, Wang J, Xie HP (2020) Anisotropic creep characteristics and mechanism of shale under elevated deviatoric stress. J Petrol Sci Eng. https://doi.org/10.1016/j.petrol.2019.106670

Li K, Yin ZY, Han D et al (2021a) Size effect and anisotropy in a transversely isotropic rock under compressive conditions. Rock Mech Rock Eng 54:4639–4662. https://doi.org/10.1007/s00603-021-02558-0

Li LL, Guan JF, Xiao ML et al (2021b) Three-dimensional creep constitutive model of transversely isotropic rock. Int J Geomech. https://doi.org/10.1061/(asce)gm.1943-5622.0002111

Lin H, Zhang X, Cao R et al (2020) Improved nonlinear burgers shear creep model based on the time-dependent shear strength for rock. Environ Earth Sci. https://doi.org/10.1007/s12665-020-8896-6

Liu W, Zhang S, Chen L (2021a) Time-dependent creep model of rock based on unsteady fractional order. J Min Safety Eng 38:388–395

Liu WW, Chen JX, Luo YB et al (2021b) Deformation behaviors and mechanical mechanisms of double primary linings for large-span tunnels in squeezing rock: a case study. Rock Mech Rock Eng 54:2291–2310. https://doi.org/10.1007/s00603-021-02402-5

Nomikos P, Rahmannejad R, Sofianos A (2011) Supported axisymmetric tunnels within linear viscoelastic burgers rocks. Rock Mech Rock Eng 44:553–564. https://doi.org/10.1007/s00603-011-0159-0

Pouragha M, Eghbalian M, Wan R (2020) Micromechanical correlation between elasticity and strength characteristics of anisotropic rocks. Int J Rock Mech Min Sci. https://doi.org/10.1016/j.ijrmms.2019.104154

Saroglou H, Tsiambaos G (2008) A modified hoek-brown failure criterion for anisotropic intact rock. Int J Rock Mech Min Sci 45:223–234. https://doi.org/10.1016/j.ijrmms.2007.05.004

Shen PW, Tang HM, Zhang BC et al (2021) Investigation on the fracture and mechanical behaviors of simulated transversely isotropic rock made of two interbedded materials. Eng Geol. https://doi.org/10.1016/j.enggeo.2021.106058

Shi XC, Yang X, Meng YF et al (2016) Modified hoek-brown failure criterion for anisotropic rocks. Environ Earth Sci. https://doi.org/10.1007/s12665-016-5810-3

Sun XM, Zhao CW, Tao ZG et al (2021) Failure mechanism and control technology of large deformation for muzhailing tunnel in stratified rock masses. Bull Eng Geol Environ 80:4731–4750. https://doi.org/10.1007/s10064-021-02222-5

Wang XG, Huang QB, Lian BQ et al (2018a) Modified nishihara rheological model considering the effect of thermal-mechanical coupling and its experimental verification. Adv Mater Sci Eng. https://doi.org/10.1155/2018/4947561

Wang ZC, Zong Z, Qiao LP et al (2018b) Elastoplastic model for transversely isotropic rocks. Int J Geomech. https://doi.org/10.1061/(asce)gm.1943-5622.0001070

Wang ZC, Zong Z, Qiao LP et al (2018c) Transversely isotropic creep model for rocks. Int J Geomech. https://doi.org/10.1061/(asce)gm.1943-5622.0001159

Wang XK, Xia CC, Zhu ZM et al (2021) Long-term creep law and constitutive model of extremely soft coal rock subjected to single-stage load. Rock Soil Mech 42:2078–2088

Wu F, Liu J, Zou QL et al (2021) A triaxial creep model for salt rocks based on variable-order fractional derivative. Mech Time-Depend Mat 25:101–118. https://doi.org/10.1007/s11043-020-09470-0

Xu GW, He C, Chen ZQ et al (2020) Transversely isotropic creep behavior of phyllite and its influence on the long-term safety of the secondary lining of tunnels. Eng Geol. https://doi.org/10.1016/j.enggeo.2020.105834

Xue D, Lu L, Yi H et al (2021) A fractional burgers model for uniaxial and triaxial creep of damaged salt-rock considering temperature and volume-stress. Chin J Rock Mech Eng 40:315–329

Yan BQ, Guo QF, Ren FH et al (2020) Modified nishihara model and experimental verification of deep rock mass under the water-rock interaction. Int J Rock Mech Min Sci. https://doi.org/10.1016/j.ijrmms.2020.104250

Zhou HW, Wang CP, Han BB et al (2011) A creep constitutive model for salt rock based on fractional derivatives. Int J Rock Mech Min Sci 48:116–121. https://doi.org/10.1016/j.ijrmms.2010.11.004